Contribution of permafrost soils to the global carbon budget

OPEN ACCESS
IOP PUBLISHING ENVIRONMENTAL RESEARCH LETTERS
Environ. Res. Lett. **8** (2013) 014026 (10pp) doi:10.1088/1748-9326/8/1/014026

Contribution of permafrost soils to the global carbon budget

Sibyll Schaphoff[1], Ursula Heyder[1], Sebastian Ostberg[1], Dieter Gerten[1], Jens Heinke[1,2] and Wolfgang Lucht[1,3]

[1] Potsdam Institute for Climate Impact Research, Telegraphenberg A62, D-14473 Potsdam, Germany
[2] International Livestock Research Institute, PO Box 30709, Nairobi, Kenya
[3] Department of Geography, Humboldt-Universität zu Berlin, Germany

E-mail: Sibyll.Schaphoff@pik-potsdam.de

Received 19 October 2012
Accepted for publication 25 January 2013
Published 19 February 2013
Online at stacks.iop.org/ERL/8/014026

Abstract
Climate warming affects permafrost soil carbon pools in two opposing ways: enhanced vegetation growth leads to higher carbon inputs to the soil, whereas permafrost melting accelerates decomposition and hence carbon release. Here, we study the spatial and temporal dynamics of these two processes under scenarios of climate change and evaluate their influence on the carbon balance of the permafrost zone. We use the dynamic global vegetation model LPJmL, which simulates plant physiological and ecological processes and includes a newly developed discrete layer energy balance permafrost module and a vertical carbon distribution within the soil layer. The model is able to reproduce the interactions between vegetation and soil carbon dynamics as well as to simulate dynamic permafrost changes resulting from changes in the climate. We find that vegetation responds more rapidly to warming of the permafrost zone than soil carbon pools due to long time lags in permafrost thawing, and that the initial simulated net uptake of carbon may continue for some decades of warming. However, once the turning point is reached, if carbon release exceeds uptake, carbon is lost irreversibly from the system and cannot be compensated for by increasing vegetation carbon input. Our analysis highlights the importance of including dynamic vegetation and long-term responses into analyses of permafrost zone carbon budgets.

Keywords: permafrost, soil carbon, climate change, dynamic global vegetation model
S Online supplementary data available from stacks.iop.org/ERL/8/014026/mmedia

1. Introduction

The permafrost zone in the high latitudes is subjected to severe climate change impacts with subsequent effects on the region's ecosystems and carbon balance. During recent decades the warming in the permafrost zone was twice as large as in the global mean (Hansen *et al* 2007), which has led to thawing events in some locations of continuous permafrost zones in Russia (Romanovsky *et al* 2010). The vegetation has also changed significantly in response to climatic changes, which has been documented by an observed increase of greenness and productivity (Lucht *et al* 2002, Walker *et al* 2012), by changes in biome composition (Chapin *et al* 2004, Wilmking *et al* 2004), an advance of tree line (Lloyd 2005), and pronounced changes in fire frequency (Chapin *et al* 2004). Changes in the water regime, such as the already observed occurrence of drought stress in association with temperature increase (Barber *et al* 2000, Wilmking *et al* 2004, Chapin *et al* 2005) will also have considerable effects on vegetation distribution in the future.

Very large amounts of carbon are stored in the northern latitudes, mostly in soils (Tarnocai *et al* 2009, Zimov *et al* 2009). Their potential release in the course of permafrost thawing will probably induce a positive feedback with the climate system. The overall carbon budget of the permafrost zone is determined by soil carbon as well as vegetation carbon dynamics and their interaction. Two aspects strongly influence the permafrost soil carbon pool. Increased vegetation growth due to warming leads to increased carbon input into the soil, whereas permafrost thawing accelerates carbon release. Among the numerous studies that have investigated the effect of global warming on permafrost, most explicitly considered the thawing of permafrost (Lawrence and Slater 2005, Dutta *et al* 2006, Anisimov 2007, Schuur *et al* 2009, Schneider von Deimling *et al* 2011). Only Koven *et al* (2011) and Schaefer *et al* (2011) were able to consider vegetation feedback. Based on the analysis of one single climate scenario, Koven *et al* (2011) suggest that the integrated carbon fluxes over the 21st century indicate a net carbon source in the permafrost zone only if microbial heating is taken into account. They demonstrate that the additional input of carbon from stimulated plant growth is able to compensate for the carbon release from soils. In contrast, Schaefer *et al* (2011) estimate a cumulative flux of about 75 Pg permafrost soil carbon into the atmosphere by 2100. Both studies did not consider changes in vegetation composition.

Using a densely spaced set of climate scenarios that systematically covers the range of uncertainties in climate patterns from 19 general circulation models (GCMs) and a rise in global mean temperature between 1.5 and 5.0 K by 2100 (Heinke *et al* 2012), we here investigate the robustness of permafrost carbon dynamics against climate change. A particular focus of this analysis is on possible future steady states of the soil carbon budget of today's permafrost zones, their main drivers, and prevailing processes. We employ the dynamic global vegetation model LPJmL (Sitch *et al* 2003, Bondeau *et al* 2007) because of its ability to reproduce the interaction of vegetation and soil carbon dynamics taking into account changes in vegetation distribution. We have extended the model by a newly developed discrete layer energy balance permafrost module, a representation of the vertical distribution of soil carbon within the soil column, and a modified soil water balance scheme.

2. Methods

2.1. Model description of LPJmL

For this study, the dynamic global vegetation model LPJmL (Sitch *et al* 2003, Bondeau *et al* 2007) has been extended by a new permafrost module. This permafrost implementation is based on a detailed energy balance, explicit freezing/thawing mechanics and an improved soil hydrology model, which goes beyond the previous implementations of Beer *et al* (2007) and Wania *et al* (2009). LPJmL explicitly simulates key ecosystem processes such as photosynthesis (Farquhar *et al* 1980, Collatz *et al* 1991, 1992, Haxeltine and Prentice 1996a, 1996b), plant and soil respiration, carbon allocation, evapotranspiration and phenology of 9 plant functional types (PFTs) representing natural vegetation at the level of biomes (Sitch *et al* 2003), and of 11 crop functional types (Bondeau *et al* 2007). The water and carbon cycles are fully coupled (Gerten *et al* 2004).

To better simulate the carbon dynamic in the permafrost zone, which is affected by vegetation growth and soil carbon decomposition, a number of model modifications have been implemented. The soil carbon decomposition rate is mainly determined by soil hydrology and soil temperature. The introduction of a newly implemented permafrost module and a new hydrology scheme has led to an improved representation of the decomposition process. Figure S2 (available at stacks.iop.org/ERL/8/014026/mmedia) shows that the model is able to simulate net ecosystem exchange (NEE) at a number of boreal fluxnet sites, which is calculated from the difference of heterotrophic respiration and net primary production (NPP). To account for different decomposition rates in the different soil layers, which is of particular importance in permafrost zones, a vertical distribution of soil carbon within the soil column following Jobbagy and Jackson (2000) has been introduced to the model. The total soil carbon amount $\mathrm{SoilC_{total}}$ is estimated from the mean annual decomposition rate $k_{\mathrm{mean}_{(i)}}$ and the mean litter input into the soil as in Sitch *et al* (2003), but is distributed to all root layers separately (equation (1)). The envisaged vertical soil distribution $\mathrm{SoilC}_{(i)}$:

$$\mathrm{SoilC}_{(i)} = \sum_{p=1}^{npft} d_{(i)}^{K_{(p)}} \mathrm{SoilC_{total}} \tag{1}$$

is estimated after a carbon equilibrium phase of 2310 years. d is the relative share of the layer i in the entire soil bucket. The slope parameters K characterize the relative rate of decrease of soil carbon content with depth for each specific PFT (p). Values are shown in table S2 (available at stacks.iop.org/ERL/8/014026/mmedia). The vertical soil distribution shown in table 4 of Jobbagy and Jackson (2000) is characterized by the soil carbon share of the respective layer and PFT $\mathrm{socfr}_{(i,p)}$:

$$\mathrm{socfr}_{(i,p)} = 10^{(K_{(p)} \log 10(d_{(i)}))}. \tag{2}$$

The mean decomposition rate for each PFT $k_{\mathrm{mean_{PFT}}_{(p)}}$ can be derived from the mean annual decomposition rate $k_{\mathrm{mean}_{(i)}}$ of the spinup years as a layer weighted value derived from equation (2):

$$k_{\mathrm{mean_{PFT}}_{(p)}} = \sum_{i=1}^{n\mathrm{layer}} (k_{\mathrm{mean}_{(i)}} \mathrm{socfr}_{(i,p)}) \tag{3}$$

$$C_{\mathrm{shift}_{(i,p)}} = \frac{\mathrm{socfr}_{(i,p)} k_{\mathrm{mean}_{(i)}}}{k_{\mathrm{mean_{PFT}}_{(p)}}}. \tag{4}$$

The annual carbon shift rates $C_{\mathrm{shift}_{(i,p)}}$ describe the organic matter input from the different PFTs into the respective layer due to cryoturbation and bioturbation and are designed for global applications.

The thermal soil characteristics are described by a heat conductance energy balance model, accounting for latent heat

from freezing and thawing of soil water:

$$\frac{\partial T_{(x,t)}}{\partial t} = \alpha \frac{\partial^2 T}{\partial x^2} \quad (5)$$

where α is thermal diffusivity, and T soil temperature at position x and time t.

Soil humidity is calculated dynamically in response to thawing and freezing, percolation of water above field capacity and transpiration of plant available water in the upper 3 m of the soil column. The first 20 cm are influenced additionally by soil evaporation. Freezing depth is calculated assuming that the fraction of frozen water is congruent with the frozen soil bucket. All newly implemented processes, which are described and evaluated in detail in the supporting information (SI available at stacks.iop.org/ERL/8/014026/mmedia), enable the dynamic consideration of soil carbon dynamics in regions affected by permafrost. Soil data describing the thermal and hydraulic characteristics are taken from the Harmonized World Soil Database (version 1.2) (2012). The original data set was first aggregated to 0.5° resolution and then classified according to the USDA soil texture classification (http://edis.ifas.ufl.edu/ss169). Hydraulic soil parameters are derived from Cosby *et al* (1984) and thermal parameters from Lawrence and Slater (2008) (see table S1 available at stacks.iop.org/ERL/8/014026/mmedia).

The model is capable of reproducing local carbon fluxes and water flux dynamics, as demonstrated in a comparison with eddy-flux tower measurements (see supplementary figures S2 and S3 available at stacks.iop.org/ERL/8/014026/mmedia). For Ameriflux and Euroflux ORNL DAAC (2011) sites of the northern latitudes above 50°N the model is able to reproduce the size and most of the variability in observed carbon and water fluxes. The observed runoff spring peak (resulting from snow melt and precipitation on still frozen ground) and interannual runoff variability in the permafrost affected river catchments is also reproduced well by the model (figure S4 available at stacks.iop.org/ERL/8/014026/mmedia). In some cases the timing is not met, which is a result of the constant value of flow velocity of 1 m s^{-1} used (Rost *et al* 2008). The quality similarity index (QSI) shows the similarity of the time series (figure S4 available at stacks.iop.org/ERL/8/014026/mmedia), especially if a time shift occurs between observation and simulation (Jachner *et al* 2007). The resulting soil carbon distribution calculated by LPJmL is shown in figure S5 (available at stacks.iop.org/ERL/8/014026/mmedia).

2.2. Climate data and simulation setup

The Climate Research Unit's (CRU) time series (TS) 3.1 data for temperature and cloud cover (Mitchell and Jones 2005) were used for model spinup and the subsequent 20th century transient run. For precipitation the Global Precipitation Climatology Centre's (GPCC) gridded precipitation data (version 5) (Rudolf *et al* 2010) was used. As the land mask for the two data sets differ, the GPCC data set was adjusted to the CRU land mask by interpolating missing cells (Heinke *et al* 2012). The number of wet days per month was created synthetically based on precipitation data using the approach by New *et al* (2000).

For the 21st century simulations climate scenarios were generated using a pattern-scaling approach (Heinke *et al* 2012). Climate patterns describing the GCM-specific changes of local temperature, precipitation and cloud cover in response to changes in global mean temperature (GMT) were extracted from the 19 GCMs which supplied data for the SRES scenarios to the World Climate Research Program's Climate Model Intercomparison Project (WCRP CMIP3). These climate patterns were scaled using GMT trajectories to create transient climate anomalies over the 21st century. GMT and corresponding greenhouse gas trajectories for temperature increases of 1.5–5.0 K above pre-industrial level by 2100 in steps of 0.5 K were generated using the reduced complexity climate model MAGICC6 (Meinshausen *et al* 2011). Transient climate anomalies were applied to a baseline climatology based on observations that deliver interannual variability. Wet days were derived synthetically from precipitation data for the historical period following the approach of New *et al* (2000). For a detailed description see (Heinke *et al* 2012).

The model runs on 0.5° × 0.5° spatial resolution using monthly input of the above described data and with global annual atmospheric CO_2 concentration from Mauna Loa station (NOAA/ESRL, www.esrl.noaa.gov/gmd/ccgg/trends/) for the historical period and with the derived CO_2 concentration from MAGICC6 for future scenarios. The model runs on a daily time step by linear interpolation of monthly data and for daily precipitation with a generator based on wet days and precipitation (Gerten *et al* 2004). The carbon equilibrium was reached after 5000 years of simulation recycling the first 30 years of the 20th century with the observed climatology as described above. Then additional 390 years were used to simulate the effects of historic land use change (Fader *et al* 2010) on the carbon budget until 1900, recycling again climate data of the years 1901–30, followed by the transient run with observed climate and land use data until 2009. As the land use data start in 1700, for the spinup time 1511–700 the land use distribution of 1700 was taken. Areas under cultivation for crop land and grazing land were included (though they are negligible in the permafrost zone), as they are required for a correct assessment of the present global carbon budget and the contribution of the permafrost zone to it. Land use was assumed to remain constant for the scenario runs.

All 152 climate scenarios (19 GCM patterns, 8 GMT trajectories) were started from the same conditions in 2010, reaching the respective GMT increase in 2100 (average of 2086–115). These runs (referred to as 'PF') were extended until 2615 with constant temperature levels and a constant atmospheric CO_2 content from the year 2100 in order to analyse equilibrium times and soil carbon stocks of long-term stabilization. A second experiment, ('PF-MH'), was conducted with the same procedure as the PF run, but assuming microbial heating of 40 MJ kgC^{-1} as suggested by Khvorostyanov *et al* (2008b) and used by Koven *et al* (2011).

A third experiment ('PF-Y') additionally accounts for deeper soil carbon deposits in soil layers below 3 m (the so-called yedoma deposits in Eastern Siberia). These were assumed to contain the same amount of carbon as the slow carbon pool of each grid cell in 2010 to accommodate the spatial distribution for the scenario period. The decomposition rate of the deep soil organic matter was parametrized with a rate of 0.025 yr^{-1} following Dutta *et al* (2006) and Zimov *et al* (2006a).

An additional experiment was conducted where change in biomass input from changed plant growth and vegetation distribution was neglected. This was implemented by running the model with static biomass input into the litter pool, allocating the average litter input of the historical period (1980–2009) to each cell and year.

3. Results and discussion

3.1. Present carbon balance and validation of ecophysiological parameters

The model results are in good agreement with independent studies of the current permafrost distribution and its active-layer thickness (figure 1). The study area, i.e. the permafrost zone, is defined to be north of 50°N and bounded by a maximum thaw depth of less than 13 m. For soil carbon stored in the upper 3 m of the permafrost zone the reported range spans from 400 Pg in a model study by Koven *et al* (2011) to 1024 Pg given by an up-scaling approach of different soil databases (Tarnocai *et al* 2009). This study estimates 952 Pg carbon in 2009, which is in the upper range, but more recent studies tend to give higher estimates (Schuur *et al* 2008). Furthermore the deep soil carbon yedoma deposits include additional 407 PgC in the deeper layer (Tarnocai *et al* 2009). The LPJmL model estimates additional 343 PgC for the PF-Y experiment, in good agreement with estimations by Zimov *et al* (2006a, 2006b), and Schuur *et al* (2008) of carbon contained in deep loess sediment accumulations below 3 m. Taking additional microbial heating into account (PF-MH), the amount of soil carbon in the pre-historic equilibrium state is quite similar to that of the PF run (carbon equilibrium was calculated as described above). Contrary to expectations, the soil carbon pool is slightly higher in PF-MH than without microbial heating, about 10 PgC in the overall permafrost zone. This is due to the thicker active layer leading to more available water for plant transpiration, and correspondingly higher plant productivity. We here focus on the experiment without additional heating as Koven *et al* (2011) have pointed out that this process shows a strong threshold behaviour and a large uncertainty due to a lack of quantitative observations.

The global land biosphere uptake modelled by LPJmL largely explains the interannual variability of the global carbon sink (figure 2). By subtracting emissions from fossil fuel combustion and cement production from the annual growth rate of atmospheric CO_2 concentration the strength of the apparent global sink can be quantified. The inferred residual terrestrial sink including land use change fluxes and ocean fluxes as suggested by Le Quéré *et al* (2009) and the terrestrial sink modelled by LPJmL (including land use

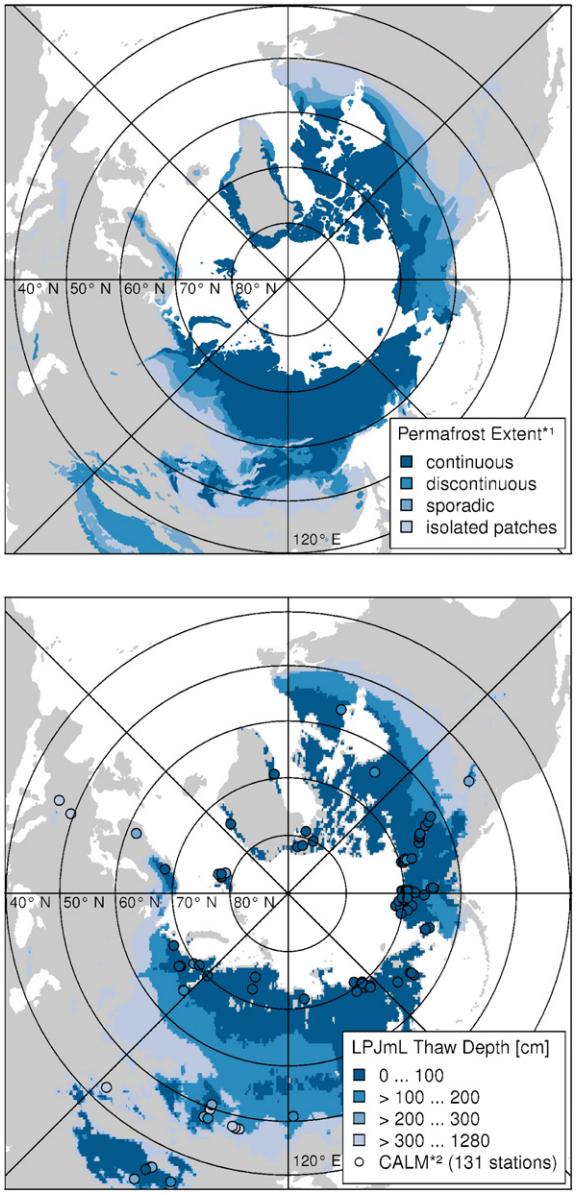

Figure 1. Observed and simulated permafrost distribution. Top, contemporary permafrost extent according to the IPA Circum-Arctic Map of Permafrost (∗[1] Brown *et al* (1998)). Bottom, LPJmL-simulated active-layer thickness in comparison with the ∗[2] CALM station data means for the monitoring time 1991–2009 (www.gwu.edu/calm/; Brown *et al* (2000)). The CALM data and the simulated thaw depth are plotted using the same colour scheme.

change emissions) are of similar magnitude and are highly correlated. The years 1991 and 1992 are the only years which cannot be explained by here simulated biosphere dynamics. Only a small increase of the atmospheric CO_2 concentration is measured in these years. Possible explanations are that the effects of the Pinatubo eruption are not included in both models or that the emission data are inaccurate due to underestimation of the collapse of industrial activity in the former eastern bloc countries especially in the year 1991 (Peters *et al* 2012). However, in the years 2000–9 both estimates of the carbon sink are in a good agreement. We estimate a loss of 7.5 Pg soil carbon globally during this

Table 1. Comparison of the estimated global terrestrial sink including land use change emission from different sources and the sink in the northern permafrost zone, for the past decades.

Terrestrial sink (Pg yr^{-1})	1981–90	1991–2000	2000–9	1981–2009
Le Quéré global sink[a]	−0.25	−1.11	−1.44	−0.89
This study global sink	−0.27	−0.63	−1.15	−0.61
This study PF sink	−0.30	−0.35	−0.55	−0.39
McGuire, Arctic sink[b]	Na	−0.27 (−0.4 to −0.2)	Na	Na

[a] Le Quéré *et al* (2009).
[b] McGuire *et al* (2009).

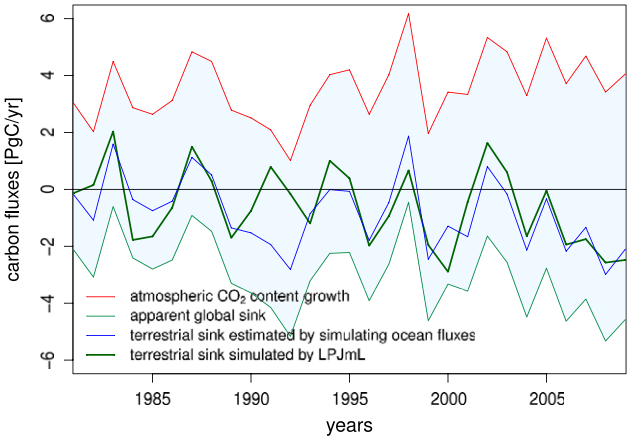

Figure 2. Estimates of the global carbon budget: the apparent sink is the difference of fossil fuel emissions and the annual growth rate of atmospheric CO_2 content (red line; data taken from www.esrl.noaa.gov/gmd/ccgg/trends/). The terrestrial sink is calculated either by adding the ocean sink (blue line; Le Quéré *et al* (2009)) or by simulations with LPJmL (dark green line) (land use emissions are included in both estimations).

period. The overall sink is largely determined by the increase of vegetation carbon which is estimated to be about 16 PgC in the years 2000–9.

More than half of the global sink is located in the permafrost zone (table 1) where our simulations show large carbon stocks. A loss of this sink would strongly affect atmospheric CO_2 concentration as less of the anthropogenic emissions would be taken up by the terrestrial biosphere. The magnitude of the land–atmosphere flux, the balance of soil respiration, fire carbon emissions and NPP, in the permafrost zone has been dominated by the increase in vegetation carbon (table 2) since the 1980s. Soil carbon has been increasing as well, but the uptake rate has been weakening. In the years 2000–2009 the soil carbon pool was almost static (see table 2) but has not yet turned into a carbon source.

3.2. Soil carbon stocks in the permafrost zone under different GMT increases and their effects on the carbon budget

Average temperatures in the study area have increased by 1.5 K since the beginning of the 20th century, which is more than the GMT increase. All climate scenarios used in this study indicate that this phenomenon of so-called polar amplification will continue during this century (table

Table 2. Contribution of the different carbon pools (Pg yr^{-1}) to the carbon budget of the permafrost zone. Positive values indicate a carbon increase.

Carbon pools	1981–90	1991–2000	2000–9	1981–2009
Vegetation	0.21	0.30	0.54	0.34
Soil	0.10	0.05	0.01	0.05

S2 available at stacks.iop.org/ERL/8/014026/mmedia). We find that for most GMT levels simulated carbon storage in permafrost soils decreases until 2100 (figure 3 and table 3). The GMT-dependent changes in soil carbon can be explained by the following mechanism. Due to increased plant productivity in response to CO_2 fertilization, longer growing periods and migration of trees into the permafrost zone, the organic matter input into the soil increases. Modelled vegetation carbon pools in the study area increase by 9–70 PgC by 2100. This is followed by an accumulation of soil carbon of 1.7–8.3 Pg in the first half of the century. After 2060, however, soil carbon pools decrease because the effect of rising temperatures on soil decomposition becomes stronger than the effect on litter input. Carbon uptake and release equalized only in the lowest temperature change scenario of 1.5 K. The slow carbon pool declines for all temperature levels, which indicates that the enhanced decomposition cannot be compensated for by increased litter input. The probability that permafrost soils turn into a carbon source is higher than 66% over all climate scenarios (including all GMT increases) and rises to 96% in both PF-Y and PF-MH experiments. The simulation of microbial heating leads to a positive feedback that increases thawing depth and accelerates the decomposition of soil organic matter. Furthermore the decomposition of the deep soil carbon deposits will lead to a much higher carbon release of more than 9 PgC until 2100 including 90% of all climate scenarios, and the median response of the 5.0 K GMT level is estimated to be more than 22 PgC. If vegetation dynamics is not taking into account the soil carbon release will be much faster (figure S6 available at stacks.iop.org/ERL/8/014026/mmedia). All scenarios start to emit carbon from the beginning of the scenario time and in 2100 at least 27 PgC is lost and carbon decrease for 5.0 K GMT increase ranges from 75 PgC to 120 PgC (figure S6 available at stacks.iop.org/ERL/8/014026/mmedia).

Additional carbon input into the soils is simulated to occur predominately in the far northern regions (figure 4)

Table 3. Projected terrestrial soil carbon changes (Pg) in the permafrost zone by 2100 for different GMT increase levels, model median (model range).

	1.5 K	2.0 K	3.0 K	4.0 K	5.0 K
PF	0.48 (−1.9 to 4.2)	−1.37 (−5.4 to 4.5)	−6.88 (−12.5 to 2.7)	−11.47 (−19.3 to 2.3)	−15.07 (−27.2 to 8.6)
PF-MH	−3.10 (−5.7 to 0.6)	−5.44 (−9.7 to 0.6)	−11.89 (−17.9 to −2.1)	−17.76 (−26.3 to −2.6)	−22.73 (−36.2 to 1.4)
PF-Y	−11.90 (−14.3 to −8.1)	−13.67 (−17.7 to −7.8)	−19.04 (−24.6 to −9.6)	−23.70 (−31.3 to −9.9)	−27.04 (−39.1 to 3.5)

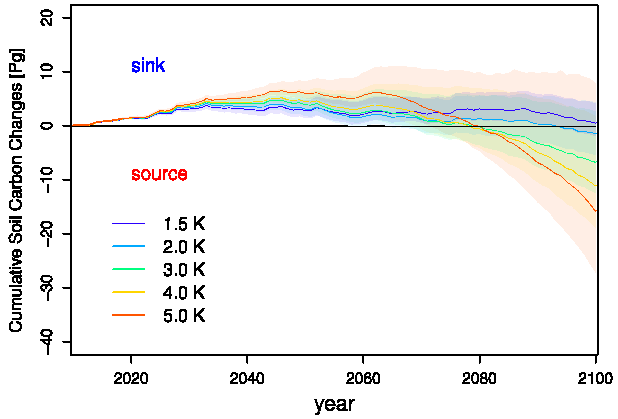

Figure 3. LPJmL-simulated cumulative soil carbon change in the permafrost zone for different levels of global mean temperature change. Transparent colours show the uncertainty ranges of 19 different GCM patterns.

where the tundra vegetation mostly represented as C3 grasses becomes more productive. North of 65°N the root zone does not thaw completely even under 5.0 K GMT increase, hence a large amount of carbon is still frozen and not released into the atmosphere until 2100. In the study area south of 60°N mean soil temperatures exceed 0 °C under all levels of GMT increase and large areas are no longer dominated by permafrost. The loss of permafrost area in 2100 at 2 K is estimated to be about 12% of the current area for 90% of all climate scenarios and twice as much for the 5 K scenarios is very likely. As a consequence, NPP increases due to increased rooting depth and higher water availability and due to an increased photosynthesis rate. Grasslands benefit most from this NPP enhancement, but this only causes a slight increase of vegetation carbon (figure 4). Trees are not able to benefit, rather a decline of tree cover is projected south of 60°N, caused by higher atmospheric water demand which cannot be fulfilled owing to the limited rooting depth of trees. Between 60°N and 75°N trees do benefit from the temperature increase, and the CO_2 fertilization effect and resulting NPP enhancement, leading to an increase of tree cover that at the beginning of the 21st century could only be found south of 60°N. Consequently, tree cover is rather homogeneous from 50°N to 70°N under the scenarios of high GMT increase.

In our simulations, the permafrost zone loses its capacity to sequester carbon under almost all considered levels of global warming (figure 5). The current sink will be amplified until 2050 but already around 2080 it will diminish or even turn into a source in 2100. Only for 3.0 K GMT increase the permafrost zone still constitutes a small sink. This is due to the increased NPP and reduced soil carbon loss at this GMT level. The lower GMT increases induce a smaller increase of NPP, for 1.5 K even a decrease, and a lower soil carbon release compared to the higher GMT levels. Both mechanisms lead to a net carbon loss of terrestrial carbon in 2100. If the soil carbon input does not change, the land–atmosphere fluxes already show a source at the beginning of the 21th century (figure S7 available at stacks.iop.org/ERL/8/014026/mmedia). The carbon source strength in 2100 reaches at least 0.25 Pg yr^{-1} and for the highest temperature scenario the carbon source rises up to 4.4 Pg yr^{-1}.

The simulation experiments for a stabilized warmer temperature show that the benefit of enhanced plant growth will not compensate for the soil carbon loss even over a longer period and the soil carbon equilibrium will be achieved at lower carbon contents for all GMT levels (figure 6). We also find that soil respiration increases for all levels of GMT increase. An equilibrium occurs much faster under low levels of warming and in the 5.0 K increase scenario soil carbon pools still decrease at the end of the simulation period after additional 500 simulation years. Consequently, all levels of GMT increase will result in a net carbon loss (figure 6), due to the delay of the thermal response in permafrost soils. In response to further thawing in the long-term, the deep soil carbon deposits (more than 3 m) are subjected to soil carbon release. This means that the response of permafrost soils to temperature increase will cause a long-term signal.

The different GMT levels also have distinct effects on vegetation and soil carbon pools (figure 7). Soil carbon storage decreases already at 1.5 K warming, although plant productivity and consequently carbon input into the soil increase at the same time. The permafrost soil carbon pool is diminished by 14 Pg at 1.5 K GMT increase and by 178 Pg at 5.0 K GMT increase for the stabilization experiment. The sensitivity of permafrost soil carbon to global warming increases non-linearly with higher temperature. As soon as vegetation becomes less productive at levels between 4.5 and 5.0 K temperature increase, vegetation carbon pools decline and soil carbon pools decline much faster than under lower temperature increases (figure 7).

4. Conclusions

We have shown that net carbon losses from permafrost soils are very likely under a wide range of future GMT

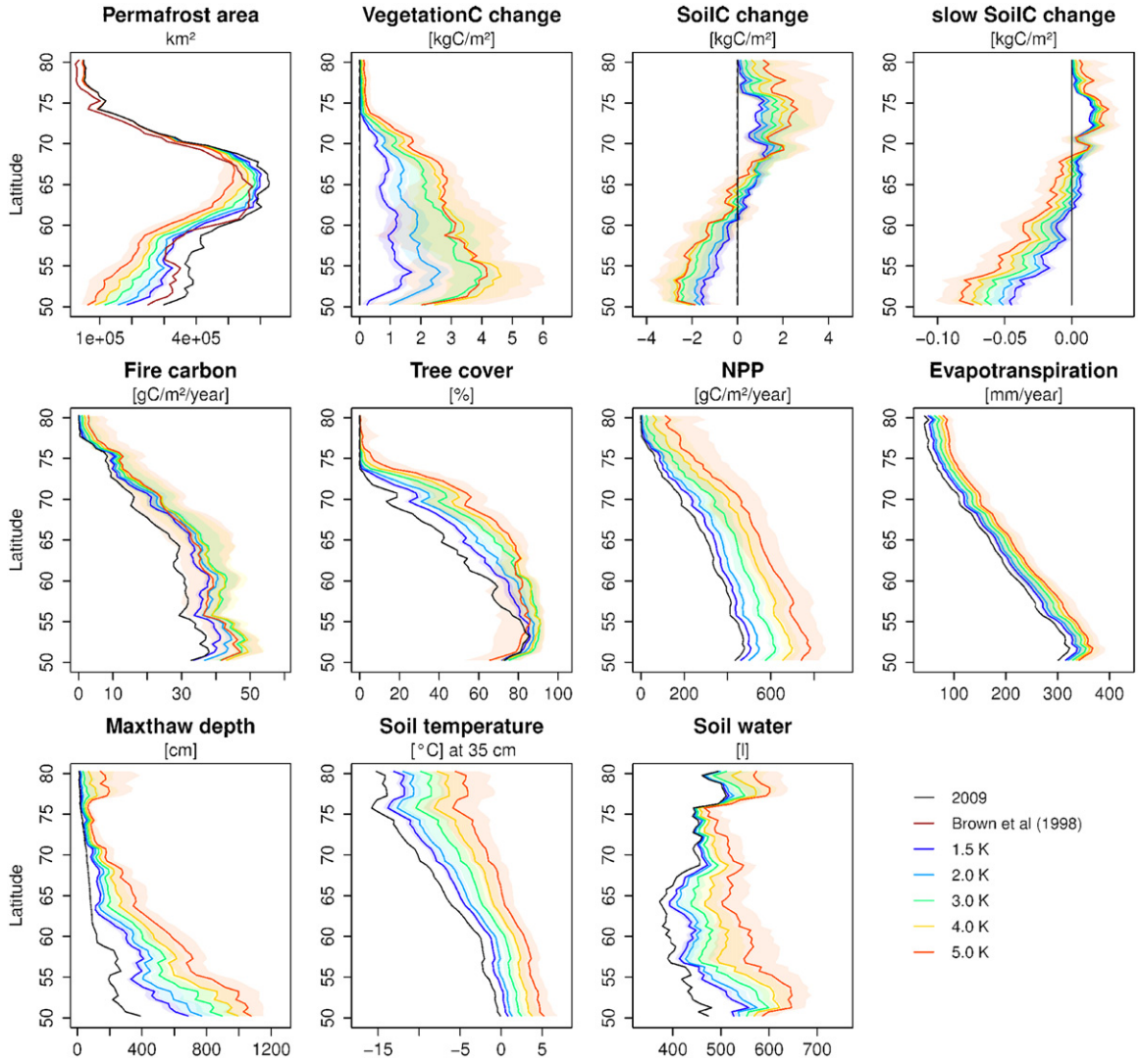

Figure 4. Changes of key ecosystem parameters in their spatial distribution in the northern hemispheric permafrost zone by 2100. The upper left plot shows the present permafrost area according to LPJmL calculations (black line) and data from Brown *et al* (1998) (brown line), and the future changes in permafrost distribution. Vegetation carbon, soil carbon and slow soil carbon pool are shown as differences compared to present conditions. Fire carbon fluxes, percentage of tree cover, net primary production, evapotranspiration, thaw depth, soil temperature and the available soil water in the rooting zone are shown as absolute values in comparison to present conditions (black lines). Transparent colours show the uncertainty ranges of 19 different GCM patterns.

rise scenarios and different spatial climate patterns (based on the analysis of 152 scenarios altogether). Although plant growth and subsequent input of organic matter may increase under global warming, even larger amounts of old soil carbon may be released into the atmosphere. Those soil carbon pools decompose very slowly and are strongly influenced by the temperature increase in the permafrost zone, especially at multi-centennial timescale. The deeper soil carbon sources amplify carbon fluxes by about the same amount as released by the additional microbial heating. The size of the latter process depends on the strength of the possible microbial heating, which is subject to large uncertainties (Khvorostyanov *et al* 2008a), and the extent of permafrost thawing, which is strongly dependent on temperature increases.

As a result of these processes operating at different timescales, the amount of carbon storage in the permafrost zone is simulated to not increase in the long-term even if plant growth continues to increase. The minimum simulated soil carbon losses by 2100 are about 2.1 Pg compared to today, but a depletion of more than 20 Pg carbon is projected for almost 70% of the considered climate projections, including all levels of GMT increase. Under 3.0 K global mean warming, a likely consequence of current emissions reductions pledges (Rogelj *et al* 2010), 60% of all climate scenarios would be associated with soil carbon losses of more than 28 Pg, equalling a rise in atmospheric CO_2 concentration by about 13 ppm. If GMT increases up to 5.0 K soil carbon losses of more than 129 Pg appear to be very likely and would increase atmospheric CO_2 concentrations by more than 60 ppm, which is almost a quarter of the pre-industrial level. Meinshausen *et al* (2011) assumed that at least 2.5 PgC of global CO_2 emissions per year will be sequestered by the ocean and the terrestrial biosphere from 2010 to 2100 for the lowest representative

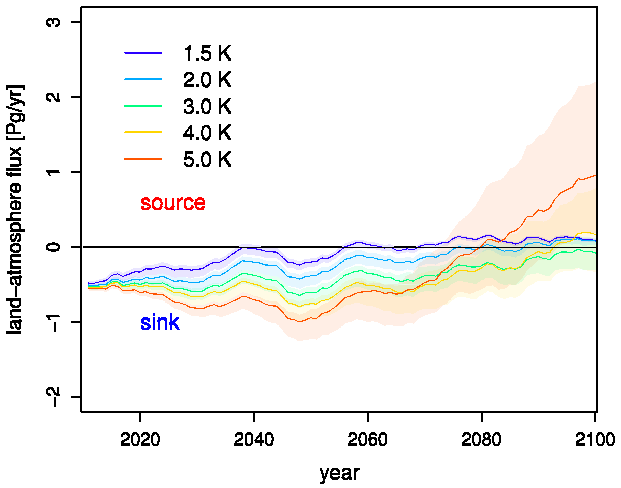

Figure 5. Land–atmosphere flux in the permafrost zone for different levels of global mean temperature change. Transparent colours show the uncertainty range of 19 different GCM patterns.

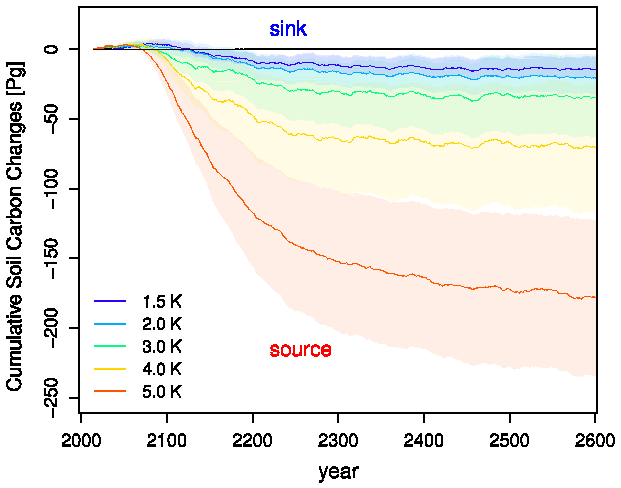

Figure 6. Cumulative soil carbon change in the permafrost zone for different levels of global mean temperature change in 2100 extended until 2600. Transparent colours show the uncertainty range of 19 different GCM patterns.

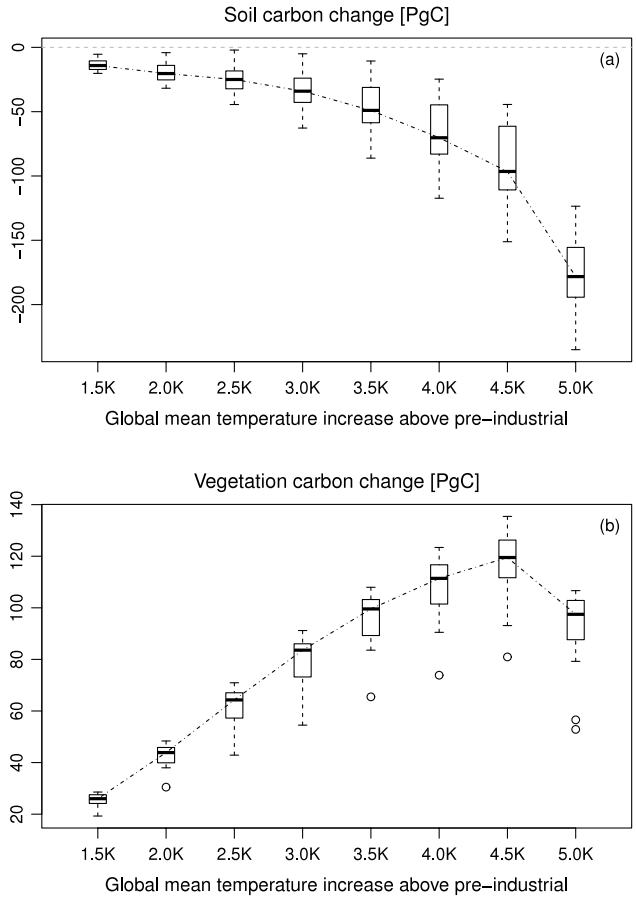

Figure 7. Long-term impacts of global mean temperature increase on soil carbon (a) and vegetation carbon (b) in the permafrost zone. Boxplots show the uncertainty ranges of 19 different GCM patterns. Dots represent individual outliers.

concentration pathway (RCP)3-PD, and up to 8 PgC yr^{-1} for the highest RCP8.5 scenario. From 1980 to 2010 the inferred sink was about 3.1 PgC yr^{-1} including the ocean and the land carbon sink and emissions from land use change. As the land carbon sink is situated predominantly in the permafrost region, the here demonstrated high likelihood that this sink will diminish or even become a net carbon source could amplify the potential warming.

The study by Koven *et al* (2011) assumes a temperature increase of about 8.0 K in the permafrost zone, which corresponds to the range of 4.0–5.0 K GMT increase of the present study (tables S2 available at stacks.iop.org/ERL/8/014026/mmedia). Their simulation experiment shows that the strength of the carbon sink decreases and at the end of the century it turns into a small source, which is comparable with this study, and in their simulation with microbial heating the permafrost zone turns into a carbon source. For the same level of temperature increase we find that the permafrost region would already turn into a net source, even when microbial heating and old deep layer carbon deposits are neglected. Taking microbial heating into account, the values are in a similar range as suggested by Koven *et al* (2011).

Our findings support the conclusion of a negative feedback of enhanced vegetation growth on the decline of soil carbon pool as suggested by process-based assumptions, which take vegetation feedback into account (Koven *et al* 2011). We show in detail that the total soil carbon amount is influenced by changes in plant productivity, especially due to changes in tree growth and tree cover decrease induced by drought stress. Especially the experiment with static carbon input into soil shows that the soil carbon balance strongly depend on the vegetation feedback due to changing climate conditions. Negative response of tree growth and increased forest mortality to warming and drought stress have already been reported for the past by Barber *et al* (2000), Wilmking *et al* (2004), Dulamsuren *et al* (2009), and Dulamsuren *et al* (2010). Our results show that this observed trend is very likely to continue in the southern permafrost zone. But also positive responses of tree growth to temperature increase were detected by Wilmking *et al* (2004), Lloyd (2005), and Lloyd and Fastie (2003), which agrees with the upward shift

and increase of tree population density in the forest–tundra ecotone simulated here.

However, the strong advance of the northern tree line and the enhanced productivity reported by the LPJmL model, but also soil carbon decomposition could be limited by nitrogen availability, which is not explicitly taken into account here. Further studies will have to address the question whether the extremely low biological nitrogen fixation in the permafrost zone (due to the energy intensity of this process and low radiation Cleveland *et al* 1999) will be overwhelmed by an enhanced energy amount and nitrogen mobilization (Melillo *et al* 2011) in a warming climate, both leading to increased nitrogen availability. Fundamental processes such as anoxic decomposition on thermokarst or on peatland could not be considered here, causing uncertainty on future high-latitude carbon balance. Pending availability of consolidated knowledge of such interacting process dynamics, the present study suggests that permafrost thawing is likely to further augment (in the medium and long-term) the climate-driven soil carbon release into the atmosphere that may be present even in the absence of such effects (Schaphoff *et al* 2006). It also suggests that even if GMT rose by up to 5.0 K, the net carbon release until 2100, and thus, the positive feedback to the global climate might be quite small relative to the first-order effects of concurrent CO_2 emissions from fossil fuel combustion.

Acknowledgments

This study was supported by the EU-FP7 research project ERMITAGE grant no. 265170, the WGL's initiative 'Pakt für Forschung', and by GLUES (Global Assessment of Land Use Dynamics, Greenhouse Gas Emissions and Ecosystem Services), a scientific coordination and synthesis project of the German Federal Ministry of Education and Research's (BMBF's) 'Sustainable Land Management' programme (Code01LL0901A). The authors are grateful to Christoph Müller and Tim Beringer for helpful comments on previous versions of this letter. We like to thank the two anonymous referee's for their very constructive annotations. Furthermore, we thank the coordinators of the FLUXNET database for the carbon and water flux data used here for validation, the Circumpolar Active Layer Monitoring (CALM) program for providing thaw depth, the National Snow and Ice Data Center (http://nsidc.org/data/docs/fgdc/ggd318_map_circumarctic/index.html) for providing Circum-Arctic Map of Permafrost, and the R-ArcticNET (www.r-arcticnet.sr.unh.edu/v4.0/index.html) for discharge data.

References

Anisimov O A 2007 Potential feedback of thawing permafrost to the global climate system through methane emission *Environ. Res. Lett.* **2** 045016

Barber V A, Juday G P and Finney B P 2000 Reduced growth of alaskan white spruce in the twentieth century from temperature-induced drought stress *Nature* **405** 668–73

Beer C, Lucht W, Gerten D, Thonicke K and Schmullius C 2007 Effects of soil freezing and thawing on vegetation carbon density in siberia: a modeling analysis with the Lund–Potsdam–Jena dynamic global vegetation model (LPJ-DGVM) *Glob. Biogeochem. Cycles* **21** GB1012

Bondeau A *et al* 2007 Modelling the role of agriculture for the 20th century global terrestrial carbon balance *Glob. Change Biol.* **13** 679–706

Brown J, Ferrians O J J, Heginbottom J A and Melnikov E S 1998 Circum-arctic map of permafrost and ground-ice conditions (Boulder, CO: National Snow and Ice Data Center) (http://nsidc.org/data/ggd318.html)

Brown J, Hinkel K M and Nelson F E 2000 The circumpolar active layer monitoring (calm) program: research designs and initial results 1 *Polar Geogr.* **24** 166–258

Chapin F S, Callaghan T V, Bergeron Y, Fukuda M, Johnstone J F, Juday G and Zimov S A 2004 Global change and the boreal forest: thresholds, shifting states or gradual change? *AMBIO* **33** 361–5

Chapin F S *et al* 2005 Role of land-surface changes in arctic summer warming *Science* **310** 657–60

Cleveland C *et al* 1999 Global patterns of terrestrial biological nitrogen (N2) fixation in natural ecosystems *Glob. Biogeochem. Cycles* **13** 623–45

Collatz G J, Ball J T, Grivet C and Berry J A 1991 Physiological and environmental regulation of stomatal conductance, photosynthesis and transpiration: a model that includes a laminar boundary layer *Agric. For. Meteorol.* **54** 107–36

Collatz G, Ribas-Carbo M and Berry J 1992 *Coupled Photosynthesis-Stomatal Conductance Model for Leaves of C4 Plants* vol 19 (Collingwood: Commonwealth Scientific and Industrial Research Organization)

Cosby B J, Hornberger G M, Clapp R B and Ginn T R 1984 A statistical exploration of the relationships of soil moisture characteristics to the physical properties of soils *Water Resour. Res.* **20** 682–90

Dulamsuren C, Hauck M, Bader M, Osokhjargal D, Oyungerel S, Nyambayar S, Runge M and Leuschner C 2009 Water relations and photosynthetic performance in Larix sibirica growing in the forest-steppe ecotone of northern Mongolia *Tree Physiol.* **29** 99–110

Dulamsuren C, Hauck M and Leuschner C 2010 Recent drought stress leads to growth reductions in Larix sibirica in the western Khentey, Mongolia *Glob. Change Biol.* **16** 3024–35

Dutta K, Schurr E A G, Neff J C and Zimov S A 2006 Potential carbon release from permafrost soils of Northeastern Siberia *Glob. Change Biol.* **12** 2336–51

Fader M, Rost S, Müller C, Bondeau A and Gerten D 2010 Virtual water content of temperate cereals and maize: present and potential future patterns *J. Hydrol.* **384** 218–31

Farquhar G D, Caemmerer S and Berry J A 1980 A biochemical model of photosynthetic CO_2 assimilation in leaves of c_3 species *Planta* **149** 78–90

Gerten D, Schaphoff S, Haberlandt U, Lucht W and Sitch S 2004 Terrestrial vegetation and water balance—hydrological evaluation of a dynamic global vegetation model *J. Hydrol.* **286** 249–70

Hansen J *et al* 2007 Dangerous human-made interference with climate: a GISS modelE study *Atmos. Chem. Phys.* **7** 2287–312

Harmonized World Soil Database 2012 *Harmonized World Soil Database (version 1.2)* (www.iiasa.ac.at/Research/LUC/External-World-soil-database/HTML/)

Haxeltine A and Prentice I C 1996a BIOME3: an equilibrium terrestrial biosphere model based on ecophysiological constraints, resource availability, and competition among plant functional types *Glob. Biogeochem. Cycles* **10** 693–709

Haxeltine A and Prentice I C 1996b A general model for the light-use efficiency of primary production *Funct. Ecol.* **10** 551–61

Heinke J, Ostberg S, Schaphoff S, Frieler K, Müller C, Gerten D, Meinshausen M and Lucht W 2012 A new dataset for

systematic assessments of climate change impacts as a function of global warming *Geosci. Model Dev. Discuss.* **5** 3533–72
Jachner S, van den Boogaart K and Petzoldt T 2007 Statistical methods for the qualitative assessment of dynamic models with time delay (R package qualV) *J. Stat. Softw.* **22** 1–31
Jobbagy E G and Jackson R B 2000 The vertical distribution of soil organic carbon and its relation to climate and vegetation *Ecol. Appl.* **10** 423–36
Khvorostyanov D V, Ciais P, Krinner G, Zimov S A, Corradi C and Guggenberger G 2008a Vulnerability of permafrost carbon to global warming. Part II: sensitivity of permafrost carbon stock to global warming *Tellus* B **60** 265–75
Khvorostyanov D V, Krinner G, Ciais P, Heimann M and Zimov S A 2008b Vulnerability of permafrost carbon to global warming. Part I: model description and role of heat generated by organic matter decomposition *Tellus* B **60** 250–64
Koven C D, Ringeval B, Friedlingstein P, Ciais P, Cadule P, Khvorostyanov D, Krinner G and Tarnocai C 2011 Permafrost carbon-climate feedbacks accelerate global warming *Proc. Natl Acad. Sci.* **108** 14769–74
Lawrence D and Slater A 2008 Incorporating organic soil into a global climate model *Clim. Dyn.* **30** 145–60
Lawrence D M and Slater A G 2005 A projection of severe near-surface permafrost degradation during the 21st century *Geophys. Res. Lett.* **32** L24401
Le Quéré C *et al* 2009 Trends in the sources and sinks of carbon dioxide *Nature Geosci.* **2** 831–6
Lloyd A H 2005 Ecological histories from alaskan tree lines provide insight into future change *Ecology* **86** 1687–95
Lloyd A H and Fastie C L 2003 Recent changes in tree line forest distribution and structure in interior Alaska *Ecoscience* **10** 176–85
Lucht W, Prentice I C, Myneni R B, Sitch S, Friedlingstein P, Cramer W, Bousquet P, Buermann W and Smith B 2002 Climatic control of the high-latitude vegetation greening trend and pinatubo effect *Science* **296** 1687–9
McGuire A D, Anderson L G, Christensen T R, Dallimore S, Guo L, Hayes D J, Heimann M, Lorenson T D, Macdonald R W and Roulet N 2009 Sensitivity of the carbon cycle in the arctic to climate change *Ecol. Monogr.* **79** 523–55
Meinshausen M, Wigley T M L and Raper S C B 2011 Emulating atmosphere–ocean and carbon cycle models with a simpler model, MAGICC6—part 2: applications *Atmos. Chem. Phys.* **11** 1457–71
Meinshausen M *et al* 2011 The RCP greenhouse gas concentrations and their extensions from 1765 to 2300 *Clim. Change* **109** 213–41
Melillo J M *et al* 2011 Soil warming, carbon–nitrogen interactions, and forest carbon budgets *Proc. Natl Acad. Sci.* **108** 9508–12
Mitchell T D and Jones P D 2005 An improved method of constructing a database of monthly climate observations and associated high-resolution grids *Int. J. Climatol.* **25** 693–712
New M, Hulme M and Jones P 2000 Representing twentieth-century space–time climate variability. Part II. Development of 1901–96 monthly grids of terrestrial surface climate *J. Clim.* **13** 2217–38
ORNL DAAC and Oak Ridge T U 2011 *Oak Ridge National Laboratory Distributed Active Archive Center (ORNL DAAC)* (http://fluxnet.ornl.gov/)
Peters G P, Marland G, Le Quéré C, Boden T, Canadell J G and Raupach M R 2012 Rapid growth in CO_2 emissions after the 2008–2009 global financial crisis *Nature Clim. Change* **2** 2–4
Rogelj J, Nabel J, Chen C, Hare W, Markmann K, Meinshausen M, Schaeffer M, Macey K and Hohne N 2010 Copenhagen accord pledges are paltry *Nature* **464** 1126–8
Romanovsky V E *et al* 2010 Thermal state of permafrost in Russia *Permafrost Periglac. Process.* **21** 136–55
Rost S, Gerten D, Bondeau A, Lucht W, Rohwer J and Schaphoff S 2008 Agricultural green and blue water consumption and its influence on the global water system *Water Resour. Res.* **44** W09405
Rudolf B, Becker A, Schneider U, Meyer-Christoffer A and Ziese M 2010 The new 'GPCC full data reanalysis version 5' providing high-quality gridded monthly precipitation data for the global land-surface is public available since December 2010 *GPCC Status Report*
Schaefer K, Zhang T, Bruhwiler L and Barrett A P 2011 Amount and timing of permafrost carbon release in response to climate warming *Tellus* B **63** 165–80
Schaphoff S, Lucht W, Gerten D, Sitch S, Cramer W and Prentice I 2006 Terrestrial biosphere carbon storage under alternative climate projections *Clim. Change* **74** 97–122
Schneider von Deimling T, Meinshausen M, Levermann A, Huber V, Frieler K, Lawrence D and Brovkin V 2011 Estimating the permafrost-carbon feedback on global warming *Biogeosci. Discuss* **8** 4727–61
Schuur E A G, Vogel J G, Crummer K G, Lee H, Sickman J O and Osterkamp T E 2009 The effect of permafrost thaw on old carbon release and net carbon exchange from tundra *Nature* **459** 556–9
Schuur E A G *et al* 2008 Vulnerability of permafrost carbon to climate change: implications for the global carbon cycle *BioScience* **58** 701–14
Sitch S *et al* 2003 Evaluation of ecosystem dynamics, plant geography and terrestrial carbon cycling in the LPJ dynamic global vegetation model *Glob. Change Biol.* **9** 161–85
Tarnocai C, Canadell J G, Schuur E A G, Kuhry P, Mazhitova G and Zimov S 2009 Soil organic carbon pools in the northern circumpolar permafrost region *Glob. Biogeochem. Cycles* **23** GB2023
Walker D A *et al* 2012 Environment, vegetation and greenness (NDVI) along the North America and Eurasia arctic transects *Environ. Res. Lett.* **7** 015504
Wania R, Ross I and Prentice I C 2009 Integrating peatlands and permafrost into a dynamic global vegetation model: 2. Evaluation and sensitivity of vegetation and carbon cycle processes *Glob. Biogeochem. Cycles* **23** GB3015
Wilmking M, Juday G P, Barber V A and Zald H S J 2004 Recent climate warming forces contrasting growth responses of white spruce at treeline in alaska through temperature thresholds *Glob. Change Biol.* **10** 1724–36
Zimov N S, Zimov S A, Zimova A E, Zimova G M, Chuprynin V I and Chapin F S 2009 Carbon storage in permafrost and soils of the mammoth tundra-steppe biome: role in the global carbon budget *Geophys. Res. Lett.* **36** L02502
Zimov S A, Davydov S P, Zimova G M, Davydova A I, Schuur E A G, Dutta K and Chapin F S 2006a Permafrost carbon: stock and decomposability of a globally significant carbon pool *Geophys. Res. Lett.* **33** L20502
Zimov S A, Schuur E A G and Chapin F S 2006b Climate change: permafrost and the global carbon budget *Science* **312** 1612–3